



Dynamic transfer auto-catalysis of epoxy vitrimers enabled by the carboxylic acid/epoxy ratio based on facilely synthesized trifunctional monoesterified cyclic anhydrides

Yanlin Liu^a, Songqi Ma^{a,*}, Qiong Li^{a,b}, Sheng Wang^{a,b}, Kaifeng Huang^a, Xiwei Xu^a, Binbo Wang^a, Jin Zhu^a

^a Key Laboratory of Bio-based Polymeric Materials Technology and Application of Zhejiang Province, Laboratory of Polymers and Composites, Ningbo Institute of Materials Technology and Engineering, Chinese Academy of Sciences, Ningbo 315201, PR China

^b University of Chinese Academy of Sciences, Beijing 100049, PR China

ARTICLE INFO

Keywords:

Vitrimer
Epoxy resins
Malleable thermoset
Dynamic transfer catalysis
Transesterification
Anhydride

ABSTRACT

Vitrimers based on transesterification exhibit reprocessable and amendable features, but highly rely on external catalyst to accelerate the stress relaxation and network rearrangement. Here we prepared reprocessable auto-catalyzed epoxy vitrimers via introducing dynamic transferrable monoesterified cyclic anhydrides into cross-linked networks. Two trifunctional monoesterified cyclic anhydrides MT and ST were facilely synthesized by catalyst-free melting reaction of maleic anhydride and succinic anhydride with trimethylolpropane, respectively, and were utilized to cure the bisphenol A epoxy DER 331. The excess monoesterified anhydrides (containing catalytic carboxyl groups) grafted in the cross-linked networks could undergo dynamic reversible reactions to transfer from one site to another, as a result, the transesterification at different sites of the networks could be effectively catalyzed. The dynamic transfer of catalytic group followed two mechanisms: i) removal-monoesterification of cyclic anhydrides and ii) transesterification of monoesterified cyclic anhydrides with hydroxyl group. In addition to the excellent reprocessability and rapid stress relaxation, the auto-catalyzed epoxy vitrimers presented high glass transition temperatures of ~ 110 °C, Young's modulus of ~ 3103 MPa and tensile strength of ~ 70.6 MPa. This dynamic transfer catalysis will provide a new idea to accelerate the stress relaxation and network rearrangement of vitrimers.

1. Introduction

Traditional thermosets are widely used as coatings, adhesives, encapsulants, and composite materials because of their excellent mechanical properties, heat resistance and solvent resistance. However, as a result of the chemically cross-linked networks, thermosets are arduous to be recycled or decomposed after curing [1–3]. For instance, once damaged or discarded, thermoset materials cannot be repaired or reprocessed by heat like thermoplastics. At present, the treatments for waste thermosetting materials are incineration and landfill, which will give rise to considerable environmental pollution and huge waste of resources.

In the interest of addressing this issue, Leibler and co-workers [4] developed the associative covalent adaptive networks (CANs) of epoxy resin based on dynamic transesterification, and pioneered the concept of vitrimer in 2011. They adopted carboxylic acids and anhydrides to cure the epoxy in

the presence of the catalyst zinc acetate ($\text{Zn}(\text{OAc})_2$). The obtained cross-linked polymers exhibited excellent mechanical and thermal properties as ordinary thermosetting resins at room temperature, while they also presented superior malleability at high temperatures, which can be attributed to the fact that a great quantity of free hydroxyl group and ester bond would proceed transesterification catalyzed by $\text{Zn}(\text{OAc})_2$. Generally, during the exchange reaction, vitrimers undergo microphase flow and stress relaxation through reversible rearrangement of dynamic covalent bonds without sacrificing material properties, which makes vitrimers combine the advantages of thermosets and thermoplastics [5]. Since then, various intriguing chemistries or dynamic covalent bonds have been explored for vitrimers or vitrimer-like materials, including transesterification [6,7], phthalate monoester transesterification [8,9], thiol-anhydride [10], vinyl-urethanes/ureas [11–14], transalkylation of triazolium salts [15], transcarbamoylation [16,17], olefin metathesis [18,19], imine exchange [20–22], disulfide exchange [23,24], siloxane [25], silyl ether [26,27],

* Corresponding author.

E-mail address: masongqi@nimte.ac.cn (S. Ma).

<https://doi.org/10.1016/j.eurpolymj.2020.109881>

Received 27 May 2020; Received in revised form 29 June 2020; Accepted 3 July 2020

Available online 10 July 2020

0014-3057/ © 2020 Elsevier Ltd. All rights reserved.

hindered urea bond [28], boroxine [29], dioxaborolane [30,31], hemiaminals [32], diselenide [33], thiol-acetal [34], diketoenamine [35], acetal [36,37], hydrazine [38], etc.

Although significant advances has been achieved for various dynamic covalent bonds, epoxy vitrimers based on dynamic transesterification are still the most studied and most promising materials because ester bond is relatively stable and the raw materials are widely available [39]. However, the reported dynamic transesterification is generally required to be accelerated with high loading of catalysts (5–10 mol%), such as organic salts [4,40,41] or strong bases [42,43]. The large amount of catalyst in vitrimers may bring about toxicity, incompatibility and corrosion issues, which will limit the application [44]. So far, there are only a few reports on the vitrimers based on transesterification without loading extra catalysts. Zhang and co-workers [44,45] disclosed epoxy vitrimers containing a large amount of free hydroxyl groups which acted as both reaction sites and catalyst to activate the dynamic transesterification. The epoxy vitrimers prepared by this method exhibited satisfactory self-healing properties. Altuna and co-workers [46] utilized citric acid to cross-link epoxidized soybean oil to prepare self-healable polymer networks. Stress relaxation took place in the absence of any extrinsic catalyst, which was also promoted by residual hydroxyl groups in the network. Ikeda and co-workers [47] reported a kind of vitrimers in which the transesterification proceeded without any catalyst, which was attributed to the high reactivity of phenyl-OH groups. Altuna and co-workers [48], Yu, Zhang and co-workers [49] incorporated tertiary amine into the network of epoxy vitrimers to catalyze the transesterification. Xu and co-workers [50] prepared a kind of epoxy vitrimers doped with carbon nanotubes or polypyrrole wrapped carbon nanotubes. In the absence of catalyst, the transesterification was accelerated by the interfacial interaction between tubular polypyrrole wrapped carbon nanotubes and epoxy. The above excellent work has laid the foundation for the research of auto-catalysis vitrimers based on transesterification. Among these transesterification-based epoxy vitrimers without catalyst addition, only Zhang and co-workers [44] mentioned the reprocessability, but the chopped samples could not avoid obvious defect even being reprocessed at 190 °C and 20 MPa. Herein, the reprocessability of auto-catalyzed epoxy vitrimers based on dynamic transesterification is still a challenge.

In this work, we innovatively introduce dynamically transferable

carboxyl group into the network of epoxy vitrimers based on transesterification to accelerate stress relaxation and network rearrangement (Fig. 1). We utilized a polyol (trimethylolpropane, TMP) to monoesterify cyclic anhydrides to synthesize trifunctional carboxylic acids which were further employed to cure a commercial epoxy (DER 331). Considering that the conjugate structure of the anhydride may affect the acidity of the obtained carboxylic acid and the performance of the cross-linked network, we used maleic anhydride (MA) and succinic anhydride (SA) as starting materials for comparison. The chemical structure of the synthesized trifunctional carboxylic acids were characterized in detail via FTIR, ^1H NMR, ^{13}C NMR and TOF-MS spectra. In addition, the curing process and kinetics as well as thermal and mechanical properties of the epoxy vitrimers were studied. Moreover, the reprocess recyclability, stress relaxation and the mechanism of dynamic transfer auto-catalysis were systematically investigated.

2. Experimental

2.1. Materials

Maleic anhydride (MA), succinic anhydride (SA), trimethylolpropane (TMP), zinc acetate ($\text{Zn}(\text{OAc})_2$) were purchased from Aladdin Reagent, China. Ethyl acetate, petroleum ether (boiling range: 60–90 °C) were bought from Sinopharm Chemical Reagent Co., Ltd., China. Bisphenol A epoxy monomer (DGEBA, trade name D.E.R.331, epoxide equivalent 182–192 g per eq.) was supplied by DOW Chemical Company, USA. All the chemicals were utilized as received unless otherwise indicated.

2.2. Synthesis of trifunctional monoesterified maleic anhydride (MT)

9.64 g (98.3 mmol) of MA and 4.00 g (29.8 mmol) of TMP were added to a 20 mL one-neck flask and heated to 110 °C. After the reactants were completely melted, the flask was kept at 110 °C in an oil bath for 5 h while being constantly stirred. The obtained product was washed with a mixture of ethyl acetate and petroleum ether (1:1) four times. After drying in a vacuum oven at 50 °C for 6 h, the product MT with a yield of 40% was obtained. In this study, in order to obtain the product as pure as possible, we used the solvent precipitation for four times, thus resulting in low yield. The synthetic route is illustrated in

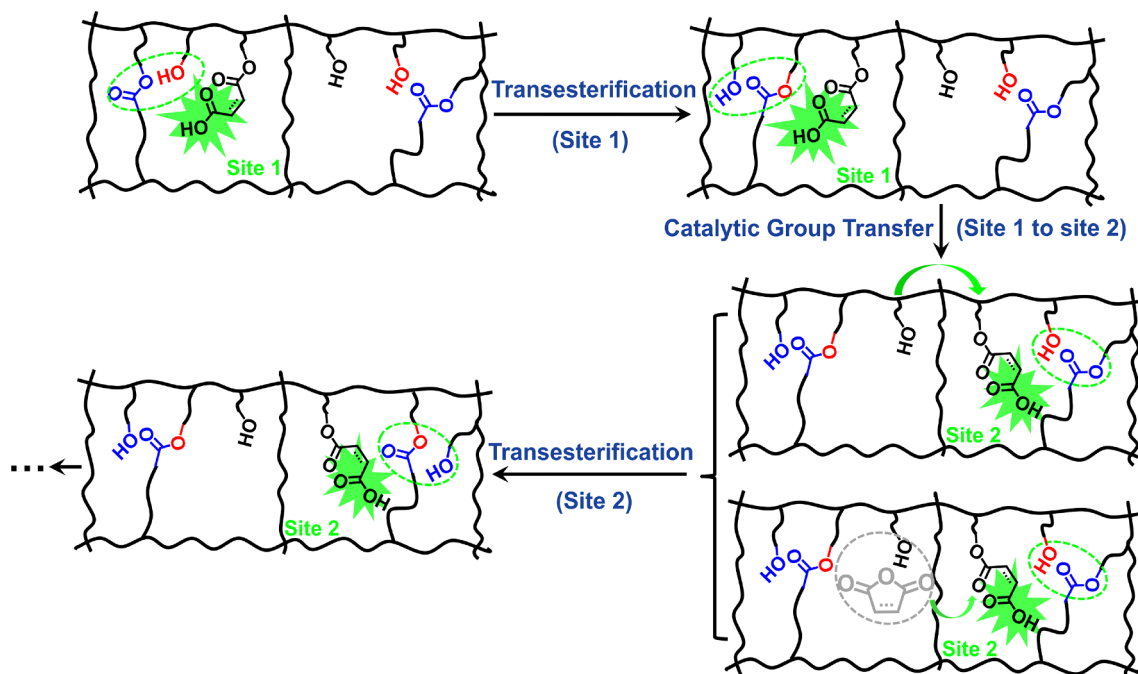
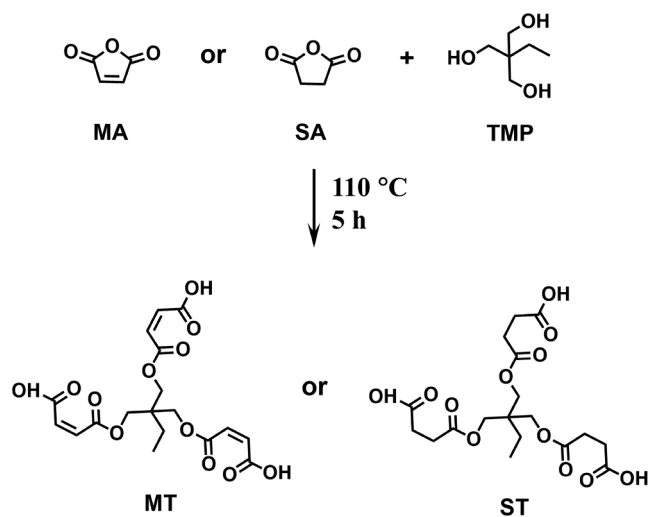


Fig. 1. Schematic diagram of dynamic transfer auto-catalytic process.



Scheme 1. Synthetic routes of MT and ST.

Scheme 1. To ensure the complete involvement of $-OH$ groups in TMP in the reaction, excess anhydride was loaded. [51,52] After reaction for 5 h, the product was purified and characterized by FTIR, 1H NMR, ^{13}C NMR and TOF-MS. TOF-MS (m/z): 427.0823. FTIR (cm^{-1}): 1700 (C=O, ester), 1750–1850 (C=O, anhydride). 1H NMR (400 MHz, Acetone- d_6 , ppm): 0.86–0.93 (t, 3H, $-CH_3$), 1.47–1.61 (q, 2H, $-CH_2-CH_3$), 4.17 (s, 6H, $-O-CH_2-$), 6.37–6.44 (dd, 6H, $-CH=CH-$). ^{13}C NMR (400 MHz, DMSO- d_6 , ppm): 7.66, 22.63, 41.02, 64.51, 128.48, 132.33, 165.31, 167.10.

2.3. Synthesis of trifunctional monoesterified succinic anhydride (ST)

9.84 g (98.3 mmol) of SA and 4.00 g (29.8 mmol) of TMP were added to a 20 mL one-neck flask and heated to 110 °C. After the reactants were completely melted, the flask was kept at 110 °C in an oil bath for 5 h while being constantly stirred. The obtained product was washed with a mixture of ethyl acetate and petroleum ether (1:1) four times. After drying in a vacuum oven at 50 °C for 6 h, the product MT with a yield of 45% was obtained. In this study, in order to obtain the product as pure as possible, we used the solvent precipitation for four times, thus resulting in low yield. The synthetic route is shown in Scheme 1. TOF-MS (m/z): 433.1292. FTIR (cm^{-1}): 1700 (C=O, ester), 1750–1850 (C=O, anhydride). 1H NMR (400 MHz, Acetone- d_6 , ppm): 0.87–0.91 (t, 3H, $=CH_3$), 1.49–1.54 (q, 2H, $=CH_2=CH_3$), 2.58–2.65 (m, 6H, $=CH_2=CH_2=$), 4.06 (s, 6H, $=O=CH_2=$). ^{13}C NMR (400 MHz, DMSO- d_6 , ppm): 7.38, 22.81, 29.09, 29.19, 41.03, 63.87, 172.31, 173.76.

2.4. Preparation of epoxy vitrimers

For the MT or ST cross-linked epoxy vitrimers (MTEs or STE-1.25), the synthesized trifunctional carboxylic acid (MT or ST) was uniformly mixed with bisphenol A epoxy (DER 331) using a homogenizer and cured without any solvent or catalyst. Different molar ratios of carboxyl group to epoxy group (0.75, 1, 1.25) were selected to prepare different MT cross-linked epoxy vitrimers (MTE-0.75, MTE-1 and MTE-1.25). For the MT cross-linked epoxy vitrimer containing catalyst $Zn(OAc)_2$ (MT-CAT-1.25), $Zn(OAc)_2$ (5 mol% relative to the COOH groups) was dissolved in MT to volatilize acetic acid before mixing with epoxy (molar ratio of carboxyl group to epoxy group was 1.25). For all the samples, bubbles were removed from the mixtures in a vacuum oven. After being poured into the mold, all the samples were cured at 90 °C for 3 h, 120 °C for 1 h, 150 °C for 2 h, 180 °C for 4 h. The feed composites of all the samples are listed in Table 1.

Table 1

Compositions of the epoxy vitrimers made using DER 331.

| Sample | Curing agent | carboxyl group/epoxy group molar ratio | catalyst $Zn(OAc)_2$ mol % |
|--------------|--------------|--|----------------------------|
| MTE-0.75 | MT | 0.75 | 0 |
| MTE-1 | MT | 1.00 | 0 |
| MTE-1.25 | MT | 1.25 | 0 |
| MTE-CAT-1.25 | MT | 1.25 | 5 |
| STE-1.25 | ST | 1.25 | 0 |

2.5. Gel content test

The samples (0.5 g) were respectively put into the Soxhlet extractor to extract with acetone for 48 h, and then dried in a vacuum oven at 70 °C for 12 h. m_0 is the initial mass, m_1 is the final mass after drying; the gel content is calculated by m_1/m_0 .

2.6. Water absorption

Due to our limited samples, irregularly shaped samples with thickness of 300–400 μm and weight of 15–20 mg were used to determine the water absorption. The samples were separately immersed in distilled water at 23 °C for 24 h. The mass before immersion was recorded as m_a . After soaking, the samples were taken out and wiped to remove surface water quickly and weighed as m_b . The water absorption was calculated by $(m_b - m_a)/m_a$.

2.7. Reprocessing recycle

The reprocess recycling test was performed in a plate vulcanizer. The films were cut into small pieces and placed between two steel sheets covered with two polyimide films to avoid resins adhering on the steel sheets. Hot pressing was implemented at 200 °C under a pressure of 10 MPa for 2 h. After cooling to room temperature, reprocessed films were obtained.

2.8. Characterizations

Fourier transform infrared (FTIR) spectra were obtained using a Micro-FTIR Cary 660 spectrometer (Agilent, America) and the absorbance mode was applied. 1H NMR and ^{13}C NMR spectra were recorded on AVANCE III Bruker NMR spectrometer (Bruker, Switzerland) using DMSO- d_6 and Acetone- d_6 as the solvents. TOF-MS spectra were measured using a Triple TOF 4600 time of flight mass spectrometer (AB Sciex, America). The temperature-dependent FTIR measurements were measured with a NICOLET 6700 (Thermo, America) using the KBr pellet method from 25 to 250 °C. Differential scanning calorimetry (DSC1, Mettler-Toledo, Switzerland) was utilized to determine the T_g values and investigate the curing behavior. The epoxy mixtures (around 3–5 mg) were taken for the study of non-isothermal curing kinetics. A heat scan ranging from 25 to 250 °C was performed at varying heating rates of 5, 10, 15, and 20 °C/min, respectively. The glass transition temperature (T_g) was obtained from the second heating curve scanned from 25 °C to 180 °C at a heating rate of 20 °C/min under a N_2 atmosphere. The thermal stability was determined using a thermogravimetric analyzer (TGA, TGA/DSC1, Mettler-Toledo, Switzerland). The samples (~6 mg) were heated from 50 to 800 °C at a heating rate of 10 °C/min under a N_2 atmosphere. The dynamic mechanical properties were characterized by a dynamic mechanical analyzer (DMA, Q800, TA Instruments, America) in the film tensile mode. The samples with dimensions of 30 mm \times 5 mm \times 0.3 mm were scanned from -50 to 180 °C at a heating rate of 3 °C/min and at a frequency of 1 Hz. Stress relaxation experiments were also tested by DMA (DMA, Q850, TA

Instruments, America). The samples with dimensions of 30 mm \times 5 mm \times 0.3 mm were initially preloaded by 1×10^{-3} N force to maintain straightness. After reaching the testing temperature, it was allowed 10 min to reach thermal equilibrium. The specimen was stretched by 1.5% on the DMA machine and the deformation was maintained throughout the test. The decrease of the stress as the function of time was recorded. The tensile properties were tested on a Universal Mechanical Testing Machine (Instron 5569A, Instron, America). In order to avoid defects during cutting, the networks were cut into easy-to-cut rectangular samples to test the tensile properties. The samples with dimensions of 30 mm (length) \times 5 mm (width) \times 0.3 mm (thickness) were measured at a cross-head speed of 1 mm/min. At least four repeated measurements were performed for each sample.

3. Results and discussion

3.1. Curing process

Fig. 2a presents the non-isothermal DSC curves of the different curing systems at the heating rate of 15 °C/min. The exothermic peaks in the DSC curves are mainly due to the reaction between the carboxyl group and the epoxy group. It can be seen that the curing reactions of DER 331 with MT occurred at lower temperature ranges than that of ST. The peak exothermic temperature (T_p) of MTE-1.25 is 27.7 °C lower than that of STE-1.25 (Table S1). This means that MT possesses higher curing reactivity toward epoxy than ST, which is attributed to the stronger acidity of the conjugated carboxyl group in the MT structure. Besides, increasing the MT amount or adding Zn(OAc)₂, the exothermic peak of the curing reaction moved to lower temperatures, which indicates that raising carboxyl concentration and introducing Zn(OAc)₂ can promote the curing reaction to a certain extent.

In order to quantitatively predict the curing reactivity of MT/ST toward DER 331, the non-isothermal curing kinetics were employed by DSC. Kissinger's method (Eq. (1)) and Ozawa's method (Eq. (2)) were utilized to compute the apparent activation energy during the curing process [53–55].

$$-\ln(\beta/T_p^2) = E_a/RT_p - \ln(AR/E_a) \quad (1)$$

$$\ln\beta = -1.052 \times E_a/RT_p + \ln(AE_a/R) - \ln F(x) - 5.331 \quad (2)$$

where β is the heating rate, T_p is the peak exothermic temperature, E_a is an average activation energy of the curing reaction, A is the pre-exponential factor, R is the gas constant, and $F(x)$ is a conversion dependent term. Fig. 2b exhibits the plots of $\ln\beta$ versus $1000/T_p$ based on Ozawa's method. The plots of $-\ln(\beta/T_p^2)$ versus $1000/T_p$ based on Kissinger's method are exhibited in Fig. S7. The T_p s and E_a s calculated from the slope of linear fitting plots are summarized in Table S1. The E_a value sequence of each sample is as follows: MTE-CAT-1.25 < MTE-1.25 < MTE-1 < MTE-0.75 < STE-1.25. As we know, the smaller the E_a value, the higher the probability that the curing reaction will occur [55]. The quantitative calculations are consistent with the results in Fig. 2a. The stronger acidity of MT makes it more likely to react with epoxy. Besides, Zn(OAc)₂ can also catalyze the curing reaction.

To obtain the optimal curing conditions, real-time FTIR was adopted to monitor the chemical change during heating. The changes of the epoxy group during heating for sample MTE-1.25 and STE-1.25 are shown in Fig. 2c and d, respectively. As the reaction occurred, the characteristic peak of epoxy group at 914 cm⁻¹ gradually weakened, and disappeared when the temperature was increased to 180 °C. Therefore, in order to ensure the completion of the reaction, the post-curing temperature for each sample was set to 180 °C and maintained for 4 h.

Gel content is a proof of the formation of a well-cross-linked network and is closely related to the properties of the thermoset. Thus, the

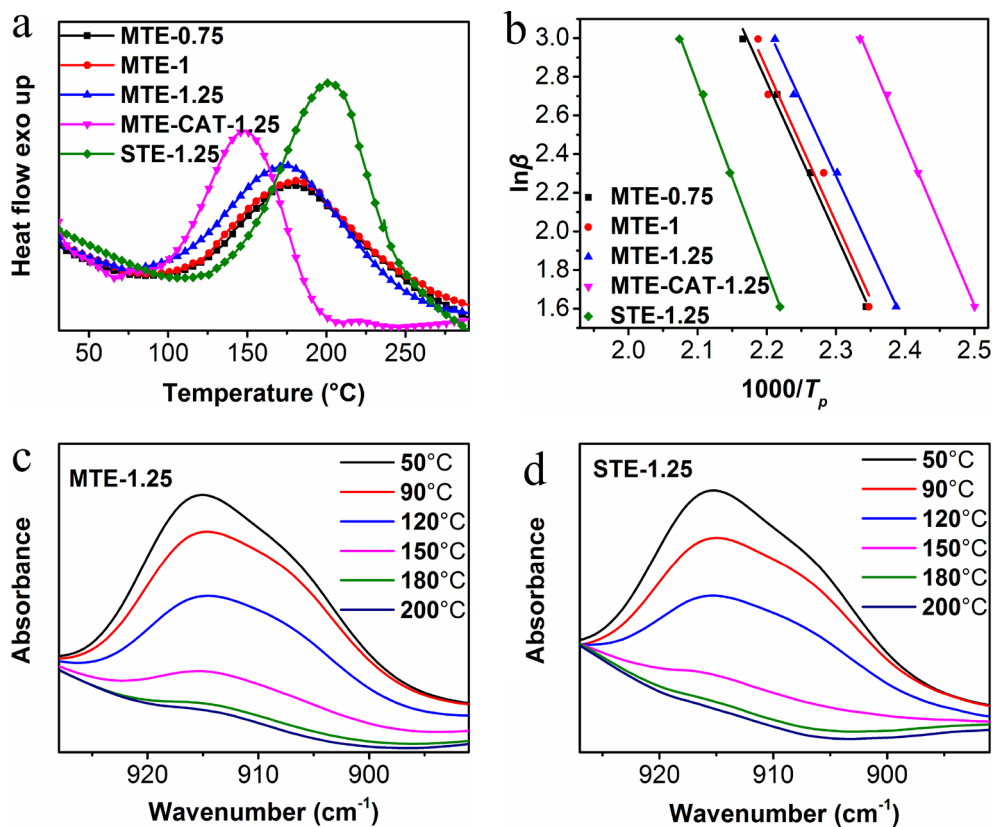


Fig. 2. (a) DSC curves of each sample at heating rate of 15 °C/min. (b) $\ln\beta$ as a function of $1000/T_p$ based on Ozawa's theories. (c,d) Epoxy regions (900–930 cm⁻¹) of temperature-dependent FTIR spectra at the heating rate of 2.5 °C/min during the curing of epoxy-acid networks (c) MTE-1.25 and (d) STE-1.25.

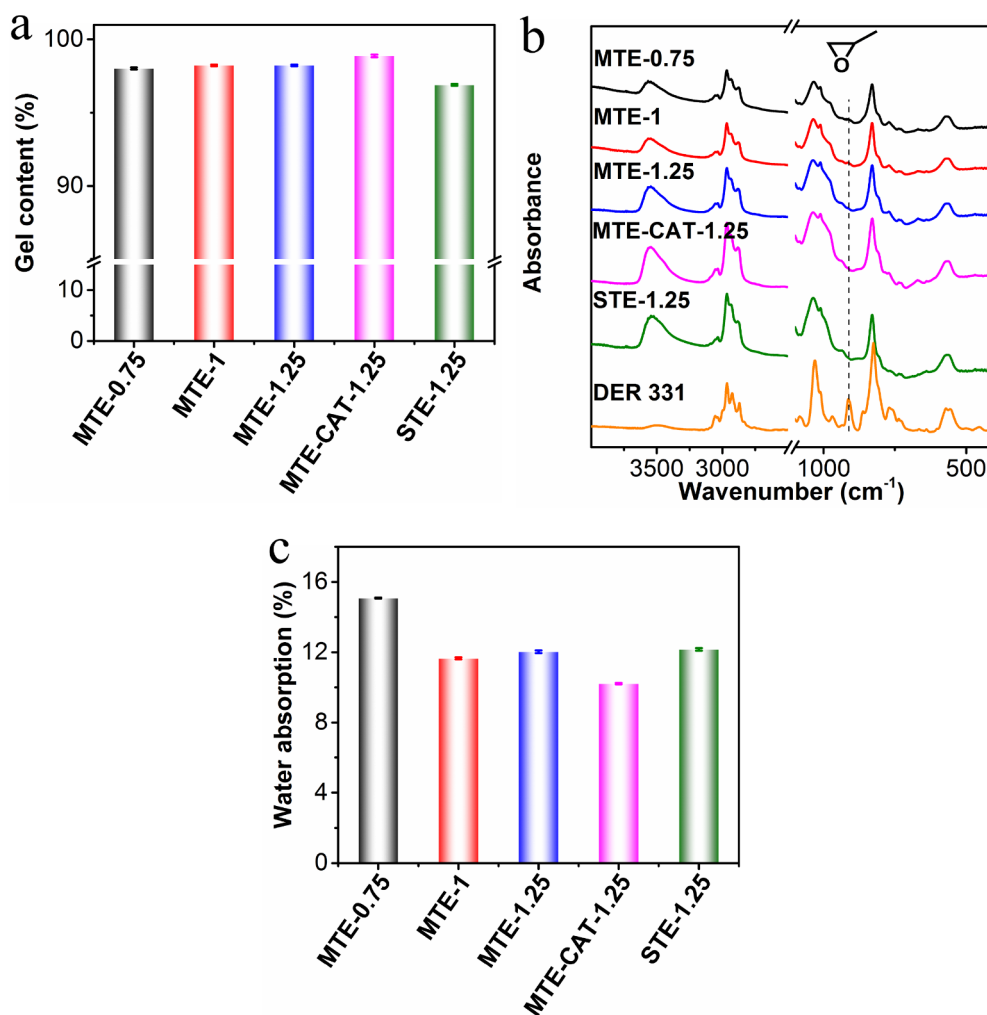


Fig. 3. (a) Gel contents, (b) FTIR spectra and (c) Water absorption of the epoxy vitrimers.

gel contents of all the cured samples were examined and presented in Fig. 3a. Each sample has a high gel content of 96.9%–99.1%, indicating that the networks were well cross-linked. To further confirm the curing degree, the FTIR spectra of each sample after curing were measured and illustrated in Fig. 3b. The characteristic peak of epoxy group in the cross-linked networks almost disappeared, which manifests that each sample was cured well. Since the residual hydroxyl and carboxyl groups were contained in the cross-linked networks, the water absorption of each sample was also determined, which were 15.08%, 11.65%, 12.03%, 10.22% and 12.16% for MTE-0.75, MTE-1, MTE-1.25, MTE-CAT-1.25 and STE-1.25.

3.2. Thermal and mechanical properties

Fig. 4a and b shows the storage modulus and $\tan \delta$ as a function of temperature, respectively, and T_g s and storage moduli are listed in Table 2. For the cross-linked network, its T_g and modulus are closely related to cross-link density (ν_e) of the network. Thereafter ν_e , the higher T_g and modulus of the system [56,57]. Hence, ν_e s of MTEs and STE-1.25 were calculated via the following Eq. (3) [56,58].

$$\nu_e = E_R/3RT \quad (3)$$

where E_R is the storage modulus at rubbery states ($T_g + 60$ °C), R is the gas constant (8.314 J/(mol·K)) and T is the Kelvin temperature of $T_g + 60$ °C. The ν_e value of MTE-1 is higher than that of MTE-0.75, which is because more carboxyl groups reacted with epoxy groups when the molar ratio of carboxyl group to epoxy group was ≤ 1 .

However, as the molar ratio of carboxyl group to epoxy group was further increased to > 1 , the system did not possess enough epoxy groups to completely consume the carboxyl groups. Therefore, the ν_e of MTE-1.25 is lower than that of MTE-1. When catalyst $Zn(OAc)_2$ was added, Zn^{2+} could form coordination bonds with carboxyl groups, corresponding to the highest ν_e of MTE-CAT-1.25. The lower rubbery modulus of STE-1.25 with respect to MTE-1.5 corresponds to its lower cross-link density. For the epoxy vitrimers MTEs, their T_g s mainly depend on the ν_e . As a result, MTE-CAT-1.25 owns the highest T_g of 120 °C, and MTE-0.75 exhibits the lowest T_g of 103 °C. For MTE-1.25 and STE-1.25, in addition to the difference in ν_e , the rigidity of the two kinds of segmental chains also differs. The conjugated double bonds in the MT structure make it more rigid than ST. Consequently, the segmental chain of STE-1.25 is easier to move than that of MTE-1.25. As a result, the T_g of MTE-1.25 (105 °C) was much higher than that of STE-1.25 (75 °C). The non-isothermal DSC curves were also applied (Fig. 4c), and the T_g trend is consistent with that from DMA results.

Fig. 5 presents the representative tensile stress-strain curves of the auto-catalyzed epoxy vitrimers, and the detailed data are summarized in Table 3. MTEs and STE-1.25 all exhibited high strength of around 70 MPa and Young's modulus of 2474–3163 MPa. As mentioned above, modulus has a close tie with ν_e and the rigidity of the chain segment of the cross-linked polymer. The greater ν_e and the rigidity of the segment are, the higher modulus is [56,57]. As a result, the Young's modulus follows the order of MTE-1 > MTE-1.25 > MTE-0.75 > STE-1.25, which is in consistent with the T_g trend from the DMA experiments. Besides, MT and ST-based auto-catalyzed epoxy vitrimers exhibited

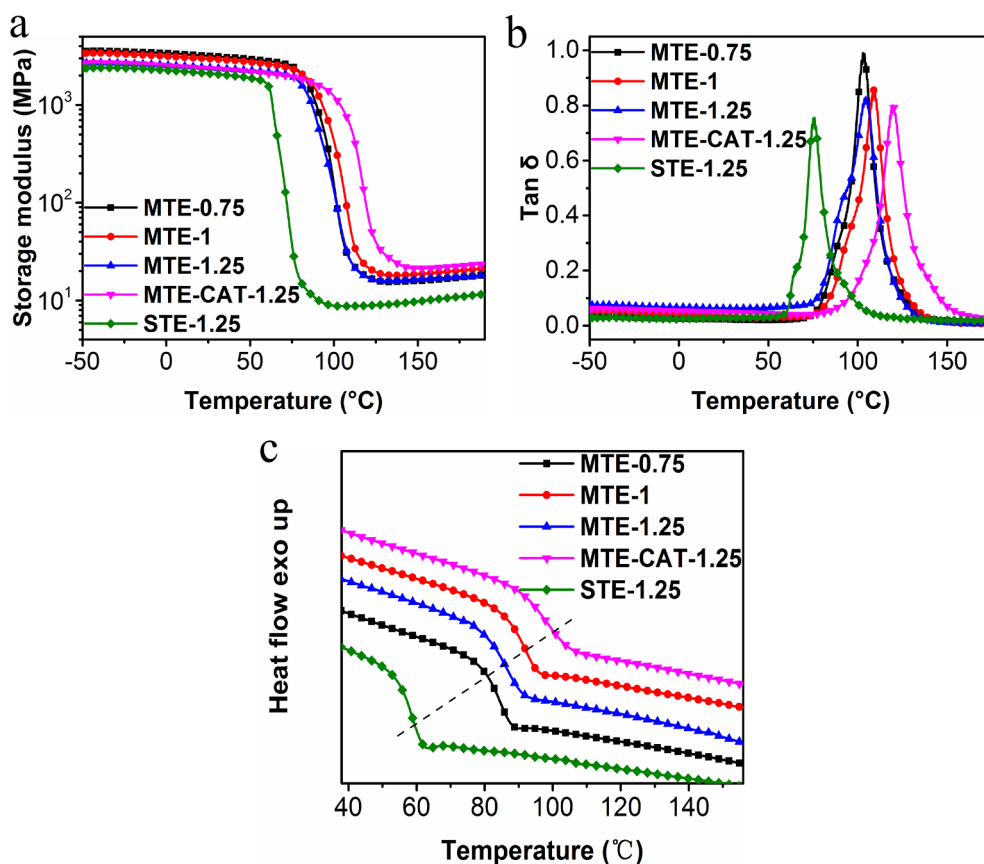


Fig. 4. (a) Storage modulus as a function of temperature for the epoxy vitrimers. (b) The tan δ as a function of temperature for the epoxy vitrimers. (c) Non-isothermal DSC curves of the epoxy vitrimers.

Table 2

Thermal properties of the epoxy vitrimers.

| Sample | T_g (°C) | | Storage modulus at $T_g + 60$ °C (MPa) | ν_e (mol/m ³) |
|--------------|------------|-----|--|-------------------------------|
| | DMA | DSC | | |
| MTE-0.75 | 103 | 83 | 16.4 | 1508 |
| MTE-1 | 110 | 91 | 19.9 | 1802 |
| MTE-1.25 | 105 | 86 | 17.9 | 1639 |
| MTE-CAT-1.25 | 120 | 98 | 22.9 | 2024 |
| STE-1.25 | 75 | 58 | 9.2 | 903 |

Table 3

Tensile properties of the epoxy vitrimers.

| Sample | Young's modulus (MPa) | Strength (MPa) | Elongation at break (%) |
|--------------|--------------------------|----------------|----------------------------|
| MTE-0.75 | 2724 ± 30 | 70.2 ± 3.0 | 6.3 ± 0.5 |
| MTE-1 | 3103 ± 30 | 68.7 ± 2.9 | 4.8 ± 0.2 |
| MTE-1.25 | 2884 ± 20 | 70.6 ± 2.1 | 5.8 ± 0.2 |
| MTE-CAT-1.25 | 2637 ± 20 | 61.8 ± 4.0 | 3.8 ± 0.5 |
| STE-1.25 | 2474 ± 50 | 67.2 ± 2.3 | 8.0 ± 0.4 |

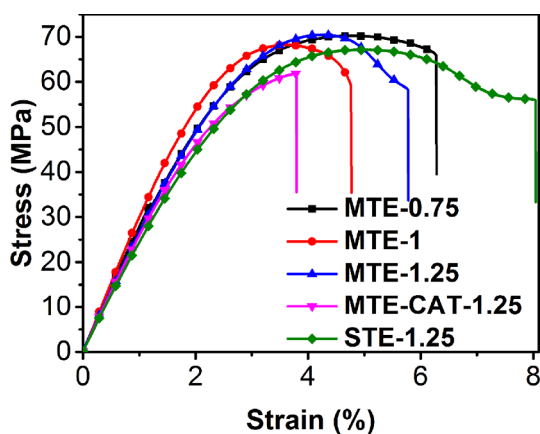


Fig. 5. Representative tensile stress-strain curves of the auto-catalyzed epoxy vitrimers.

some tough feature because they all yield before final rupture. The elongation at breaks exhibited an opposite trend of Young's moduli of MTE-1 < MTE-1.25 < MTE-0.75 < STE-1.25, which is due to the reason that elongation at break of a cross-linked polymer often decreases with the increase of ν_e and the rigidity of the chain segment. Opposite to T_g , the mechanical properties of MTE-1.25 decreased after introducing Zn(OAc)₂.

3.3. Reprocess recycling of the auto-catalyzed epoxy vitrimers

The dynamic transesterification imparts thermosets reprocessability which is a crucial feature of vitrimers. Vitrimers' reprocessability is often determined by first cutting the sample into small pieces and then reshaping it at a certain temperature and pressure. Therefore, the fast exchange reactions in the network are needed, and the reprocessing of epoxy vitrimers based on transesterification often requires the addition of catalysts [4,59,60]. Among the several existing reports of auto-catalyzed epoxy vitrimers, the transesterification was promoted by the hydroxyl group [44–47,50] and amine group [48] in the cross-linked networks, so that the networks could achieve stress relaxation and

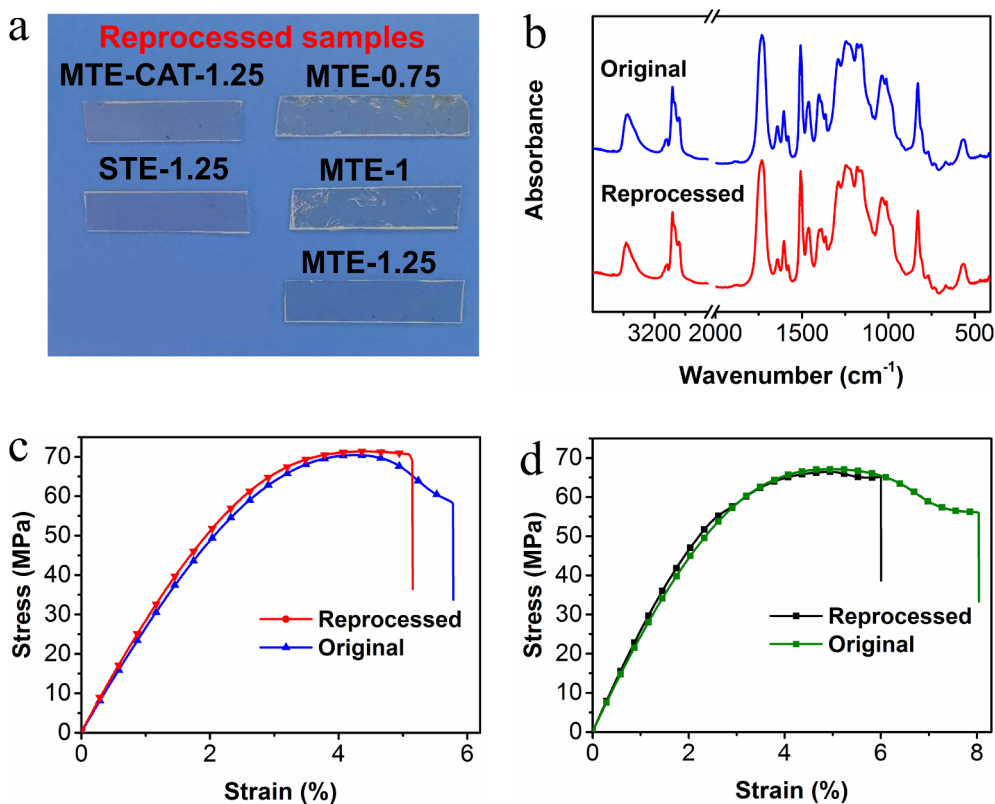


Fig. 6. (a) Appearance of the reprocessed epoxy vitrimers. (b) FTIR spectra of the original and reprocessed MTE-1.25. (c,d) Representative tensile stress-strain curves of (c) MTE-1.25 and (d) STE-1.25.

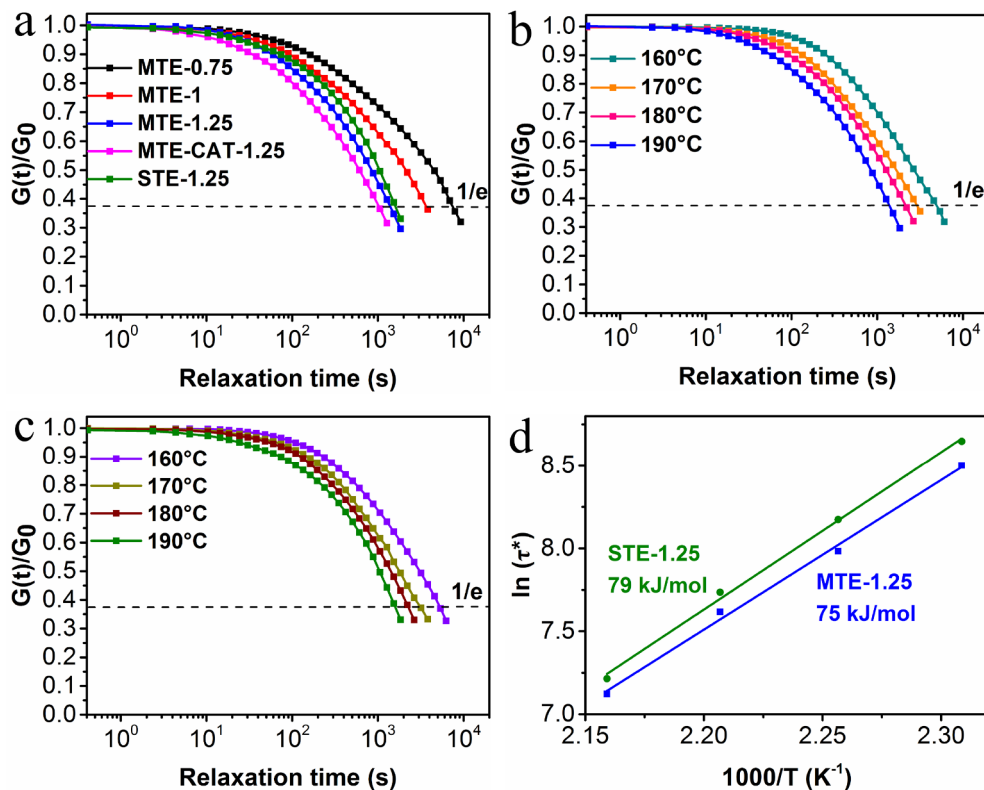


Fig. 7. (a) Modulus relaxation of each sample at 190 °C. (b, c) Modulus relaxation of MTE-1.25 (b) and STE-1.25 (c) at different temperatures. (d) Fitting of relaxation time to an Arrhenius equation.

thermal repairment. During these reports, only Zhang et al. [44] mentioned the reprocessing of the catalyst-free epoxy vitrimers, but the new film obtained via hot pressing from the pieces had a lot of cracks and weld lines which could not be avoided through increasing the compression temperature or pressure, as a result, it could not be suitable for tensile test. In this work, the thermal reprocess recyclability of the epoxy vitrimers was tested. As can be seen in Fig. 6a, the fragments of all samples reformed into wholes after hot pressing, which indicates that the transesterification occurred for each sample. However, among these reprocessed samples, only MTE-1.25, MTE-CAT-1.25 and STE-1.25 were smooth and crack-free. The reprocessed samples of MTE-0.75 and MTE-1 both had some visible cracks. The FTIR and tensile tests were performed after reprocessing. Take MTE-1.25 as an example, its characteristic peaks in the FTIR spectra (Fig. 6b) before and after reprocessing are almost the same, which indicates that the chemical structure have not been changed during reprocessing. As presented in Fig. 6c and d, the mechanical properties of MTE-1.25 and STE-1.25 were maintained extremely well after reprocessing.

3.4. Stress relaxation

For the sake of giving a theoretical basis for the results of thermal

reprocessing, the stress relaxation experiments were performed, and the results are summarized in Fig. 7. For vitrimers, dynamic exchange reactions can rearrange the cross-linked network to relax internal stress. Thus, the speed of stress relaxation depends on the speed of the exchange reaction. As can be seen in Fig. 7a, MTE-CAT-1.25, MTE-1.25 and STE-1.25 exhibited rapid stress relaxation, followed by MTE-1 and MTE-0.75, which is consistent with the results of thermal reprocessing.

The relaxation time (τ^*) is defined as the time for the modulus to reach $1/e$ (0.37) of its initial modulus. The activation energy (E_a) was calculated according to the Arrhenius equation: [61]

$$\ln \tau^* = E_a/RT - \ln A \quad (4)$$

where A is the Arrhenius prefactor, E_a is the activation energy for viscous flow, R is the gas constant, and T is the experimental temperature. An excellent fitting for both MTE-1.25 and STE-1.25 was obtained. The E_a s can be used to characterize the efficiency of dynamic transesterification. The calculated E_a s of MTE-1.25 and STE-1.25 were 75 and 79 kJ/mol, respectively. Albeit the more rigid segmental chain and higher cross-link density of MTE-1.25 than that of STE-1.25 should lead to higher E_a , MTE-1.25 exhibited a litter lower E_a than STE-1.25. This can be explained by two reasons: i) the catalytic group in the network of MTE-1.25 has higher acidity on account of the conjugation effect from

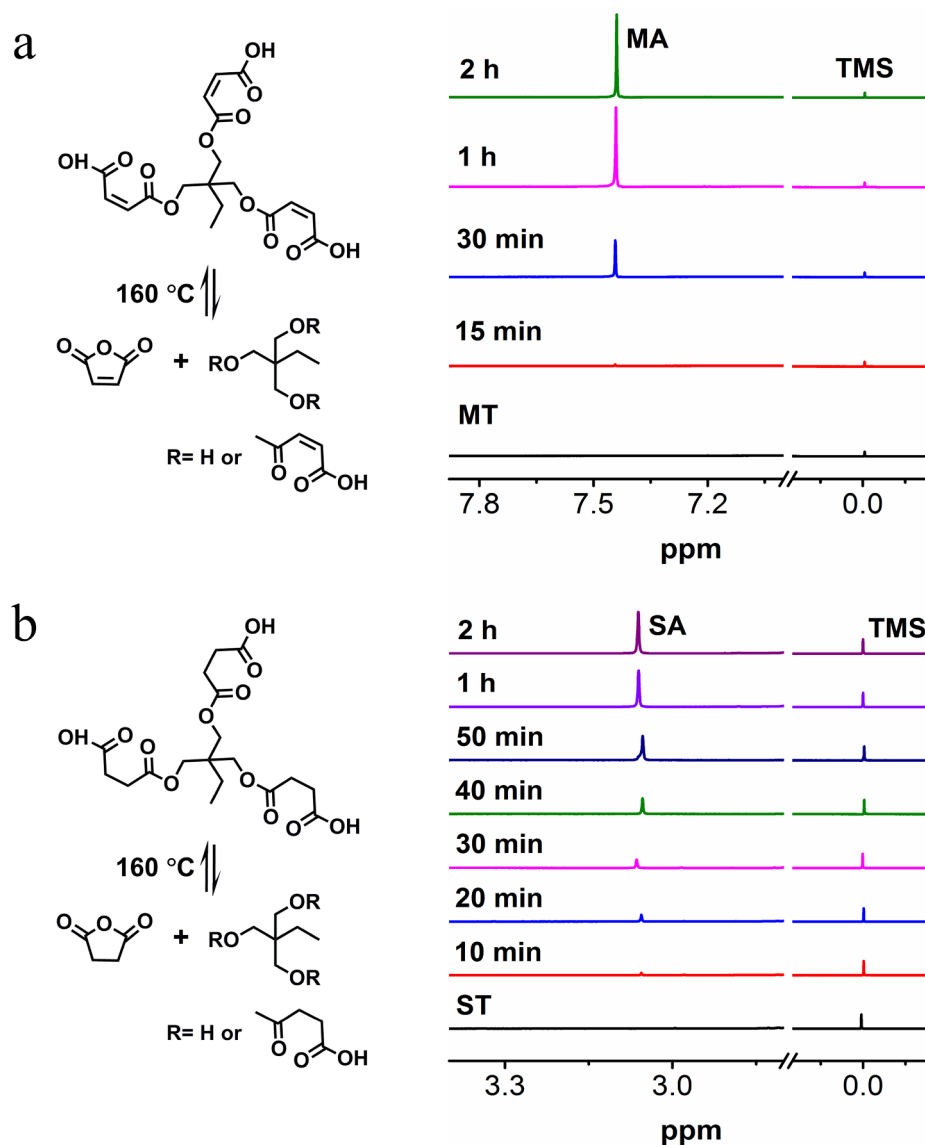


Fig. 8. Dynamic reversible reactions of MT (DMSO- d_6) and ST (acetone- d_6).

the carbon-carbon double bond, corresponding to the higher catalytic activity of MTE-1.25 than that of STE-1.25; ii) the catalytic group transferring in the network of MTE-1.25 was more likely to occur than that in the network of STE-1.25.

3.5. Mechanism of dynamic transfer auto-catalysis

According to reports [8], carboxyl groups can catalyze the transesterification, consequently carboxyl groups in the cross-linked network structure should have a certain catalytic effect. As mentioned above, MTEs (especially MTE-1.25 with excess carboxyl group) and STE-1.25 exhibited rapid stress relaxation and could be reprocessed.

During the synthesis of MT, we found that maleic anhydride (MA) could be released from the MT when it was dried in an oven at 80 °C (Fig. S9), and we all know that MA can react with the produced hydroxyl group again, so the monoesterification of MA is a dynamic reversible reaction. If the dynamic reversible monoesterification occurred in the network, the catalytic carboxyl group could be transferred from one site to other sites, which might accelerate the auto-catalysis and the network rearrangement. To confirm this assumption, the reversible reactions of MT and ST were investigated, respectively. ^1H NMR spectra were used to track the formation of maleic anhydride or succinic

anhydride to evaluate the progress of the reversible reactions. It was found that the reversible reaction of MT could be observed at temperatures of 80 °C and above (Fig. S9), and the reversible reaction of ST could also occur at temperatures of 120 °C and above (Fig. S10). The above difference might be related to the conjugate structure of MT. The ^1H NMR spectra of the reversible reactions of MT and ST at 160 °C are exhibited in Fig. 8. It can be seen that the amount of maleic anhydride and succinic anhydride in the system gradually increased with thermal treatment time, and both reached constant values after 1 h, which proved that MT and ST both undergone reversible reactions to remove the anhydride. To confirm that the anhydride could also be formed in the network of MTE-1.25 and STE-1.25, TGA-FTIR tests were performed on MTE-1.25 and STE-1.25 (Fig. 9). The two TGA curves showed degradation steps at around 230 °C and 280 °C, respectively (Fig. 9a). Furthermore, the FTIR spectra of the pyrolytic gases at these two temperatures demonstrated that maleic anhydride and succinic anhydride were released (Fig. 9b). Moreover, MTE-1.25 and STE-1.25 were immersed in DMSO and boiled in a 200 °C oil bath for 2 h to extract the related anhydrides. The ^1H NMR spectra of the extracts also proved that maleic anhydride and succinic anhydride could be formed in the networks at high temperatures (Fig. S13 and S14).

After the formation of anhydrides in the network has been proven, we subsequently explored the process of catalyst group transfer in the network. It's difficult to directly capture the catalyst group transfer process in the chemical cross-linked epoxy networks. Here, entangled network of polyethylene was used to stimulate the epoxy network and blended with model compounds. Butyric acid and butyl glycidyl ether were used as starting materials to synthesize a model compound containing β -hydroxyester group abbreviated as BBGE (the synthetic scheme and the ^1H NMR spectrum of BBGE were shown in Scheme S1 and Fig. S15), which was used to simulate the structure of epoxy after ring-opening in MTE-1.25. Then, BBGE and MT were blended into polyethylene by extrusion (the molar ratio of BBGE and carboxyl group in MT was 4: 1, while the mass of the mixture of MT and BBGE accounted for 15 wt% of polyethylene), where MT could simulate the residual mono-esterified anhydride in MTE-1.25. After blending, the PE-BBGE-MT mixture was hot pressed at 180 °C for 2 h via a plate vulcanizer. The state of BBGE and MT in the network during hot pressing and the reactions between the two were shown in Fig. 10, which was proved by the ^1H NMR spectrum of the extract in the network after hot pressing (Fig. 11). It can be seen from Fig. 11 that in the entangled network of PE, MT could undergo a reversible reaction to form maleic anhydride, which would further graft onto the BBGE structure. As a result, the carboxyl group was successfully transferred from one site to another. There might be two paths for the transfer of the catalytic group. One is that the monoesterified anhydride group directly undergoes the transesterification reaction with the hydroxyl group, and the other is removal and re-monoesterification of the acid anhydride during the reaction (Fig. 10a). In addition, MT (0.016 g, 0.037 mmol) and BBGE (0.1 g, 0.459 mmol) were also dissolved in a relatively large amount of DMSO (5 mL) to prepare a dilute solution to reduce the probability of collision between the two model compounds. The dilute solution was thermally treated at 180 °C for 2 h. The ^1H NMR spectrum of the mixture after reaction (Fig. S16) indicated that the monoesterified anhydride group of MT in the dilute solution had undergone a ring-closing reaction and the formed anhydride was further grafted onto the BBGE structure.

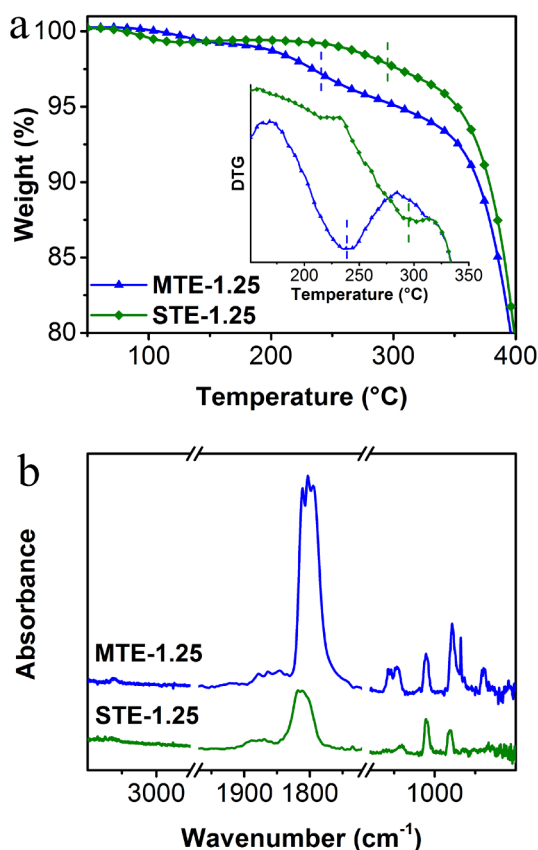


Fig. 9. TGA-FTIR curves of the epoxy vitrimers. (a) TGA curves of MTE-1.25 and STE-1.25. (b) FTIR spectra of pyrolytic gases of MTE-1.25 at 230 °C and STE-1.25 at 280 °C.

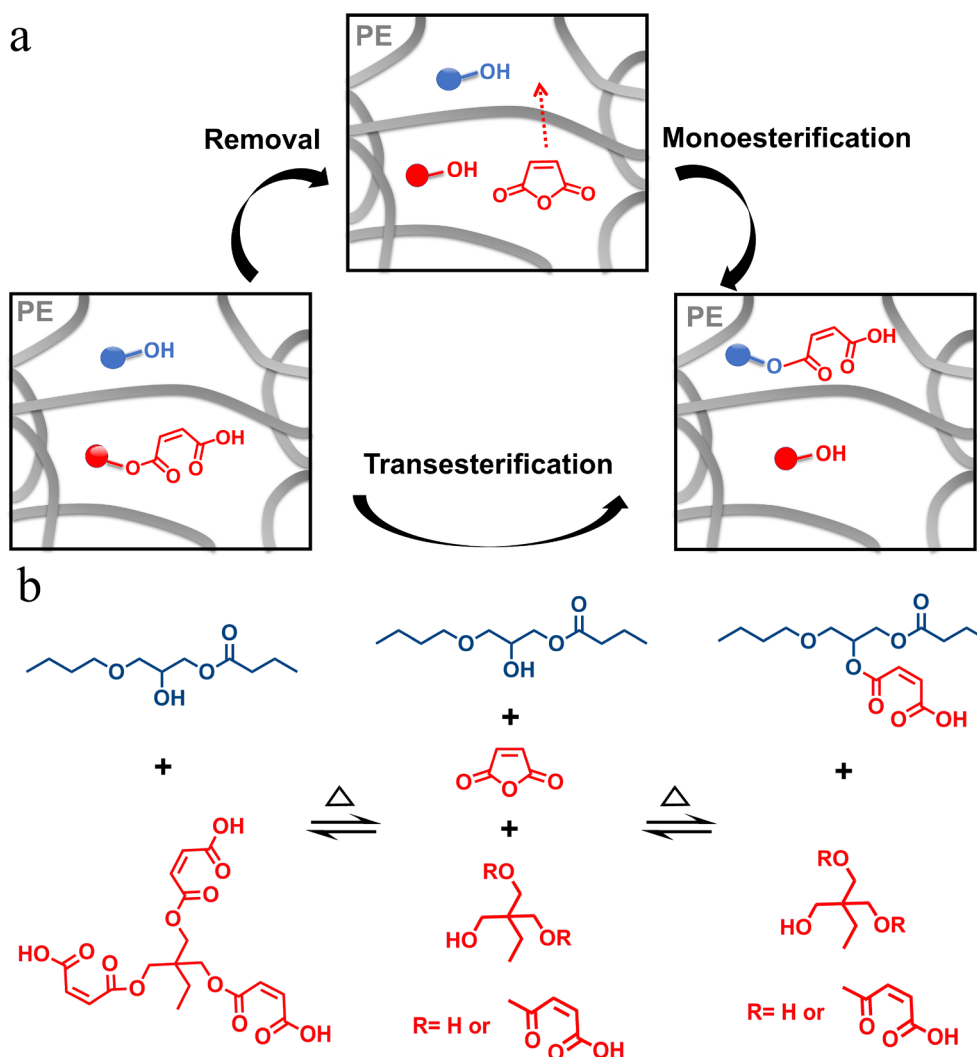


Fig. 10. Dynamic transfer of the catalytic carboxyl group in PE simulated network.

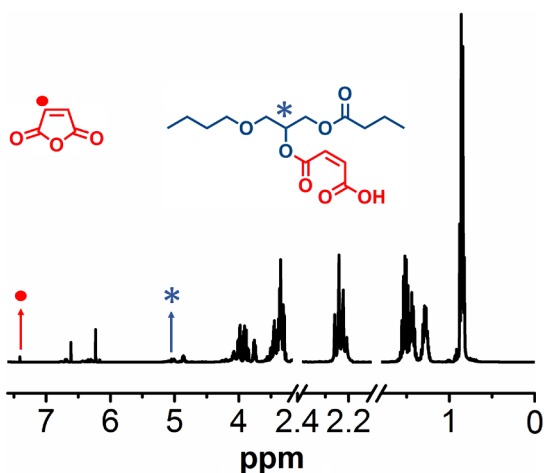
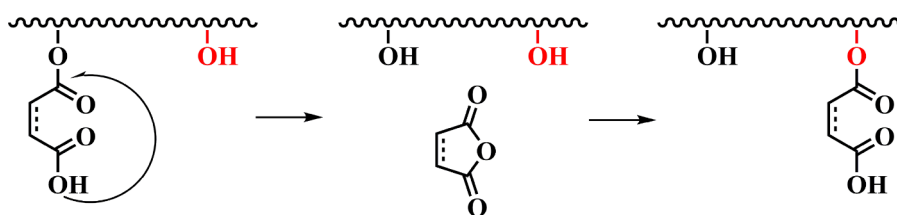


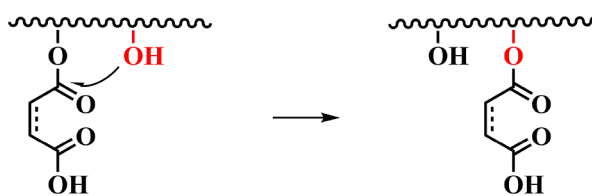
Fig. 11. ^1H NMR ($\text{DMSO-}d_6$) spectrum of the extract from the thermally treated PE simulated network.

Based on the above analysis, the dynamic transfer of catalytic carboxyl group in the MTE-1.25 and STE-1.25 may follow two mechanisms: i) removing cyclic anhydride in one site and transferring the removal anhydride and undergoing monoesterification reaction with hydroxyl groups in other sites in the network (Scheme 2a) and ii) transesterification of monoesterified cyclic anhydrides with hydroxyl group (Scheme 2b). Vitrimers exhibiting competitive mechanisms for the exchange of covalent bonds show non-linear Arrhenius plots of characteristic relaxation times, reflecting the variation of the predominant mechanism in different temperature ranges [62–64]. The characteristic relaxation times in Fig. 7(d) show linear Arrhenius relationship within the measured temperature range, indicating that the prevailing mechanism is the catalysis of transesterification by carboxylic acid groups, enhanced by the migration of these groups along the network by similar transesterification steps. The mechanism based on the regeneration of the anhydride exists, but its effect is not as significant as the transesterification mechanism.

a Removal-monoesterification of cyclic anhydride



b Transesterification



Scheme 2. Mechanism of dynamic transfer of the catalytic carboxyl group.

4. Conclusions

For the first time, dynamic transfer catalysis was explored in vitrimers, and a new type of epoxy vitrimers were successfully prepared via cross-linking bisphenol A epoxy with self-synthesized trifunctional monoesterified cyclic anhydrides. Trifunctional monoesterified maleic anhydride (MT) showed higher reactivity toward epoxy group than trifunctional monoesterified succinic anhydride (ST), and MT cross-linked vitrimers relaxed faster than ST cross-linked one. According to literature reports, auto-catalyzed vitrimers based on transesterification could relax but were exceedingly difficult to be reprocessed. In this work, reprocessing was achieved through the dynamic transfer catalysis by the monoesterified anhydrides grafted in the cross-linked networks. The dynamic transfer of catalytic group follows two mechanisms of removal-monoesterification of cyclic anhydrides and transesterification of monoesterified cyclic anhydrides with hydroxyl group. In virtue of the conjugated structure of MT, dynamic transfer catalytic process of MT cross-linked vitrimer was more obvious than ST cross-linked vitrimer. Besides, the auto-catalyzed vitrimers possessed high performance with T_g of ~ 110 °C, Young's modulus of ~ 3103 MPa and tensile strength of ~ 70.6 MPa. Dynamic transfer catalysis is a new idea for the study of vitrimers. However, how to maximize the efficiency of dynamic transfer catalysis and to achieve rapid reprocessing of vitrimers still requires further exploration.

CRedit authorship contribution statement

Yanlin Liu: Investigation, Data curation, Validation, Writing - original draft, Funding acquisition, Project administration. **Songqi Ma:** Conceptualization, Supervision, Writing - review & editing, Validation, Writing - original draft, Funding acquisition, Project administration. **Qiong Li:** Data curation. **Sheng Wang:** Data curation. **Kaifeng Huang:** Data curation. **Xiwei Xu:** Data curation. **Binbo Wang:** Data curation. **Jin Zhu:** Writing - review & editing.

Declaration of Competing Interest

The authors declare that they have no known competing financial interests or personal relationships that could have appeared to influence the work reported in this paper.

Acknowledgements

This work was financially supported by Natural Science Foundation of Zhejiang Province (No. LQ20E030005), Natural Science Foundation of Ningbo (No. 2019A610131), National Natural Science Foundation of China (No. 51773216), and Youth Innovation Promotion Association, CAS (No. 2018335).

Appendix A. Supplementary material

Supplementary data to this article can be found online at <https://doi.org/10.1016/j.eurpolymj.2020.109881>.

References

- [1] S. Ma, D.C. Webster, Degradable thermosets based on labile bonds or linkages: A review, *Prog. Polym. Sci.* 76 (2018) 65–110.
- [2] J.M. Garcia, G.O. Jones, K. Virwani, B.D. McCloskey, D.J. Boday, G.M. ter Huurne, H.W. Horn, D.J. Coady, A.M. Bintaleb, A.M.S. Alabdulrahman, F. Alsewilem, H.A.A. Almegren, J.L. Hedrick, Recyclable, strong thermosets and organogels via paraformaldehyde condensation with diamines, *Science* 344 (2014) 732–735.
- [3] X. Xu, S. Ma, J. Wu, J. Yang, B. Wang, S. Wang, Q. Li, J. Feng, S. You, J. Zhu, High-performance, command-degradable, antibacterial schiff base epoxy thermosets: synthesis and properties, *J. Mater. Chem. A* 7 (2019) 15420–15431.
- [4] D. Montarnal, M. Capelot, F. Tournilhac, L. Leibler, Silica-like malleable materials from permanent organic networks, *Science* 334 (2011) 965–968.
- [5] M. Chen, L. Zhou, Y. Wu, X. Zhao, Y. Zhang, Rapid stress relaxation and moderate temperature of malleability enabled by the synergy of disulfide metathesis and carboxylate transesterification in epoxy vitrimers, *ACS Macro Lett.* 8 (2019) 255–260.
- [6] M. Capelot, D. Montarnal, F. Tournilhac, L. Leibler, Metal-catalyzed transesterification for healing and assembling of thermosets, *J. Am. Chem. Soc.* 134 (2012) 7664–7667.
- [7] A. Legrand, C. Soulié-Ziakovic, Silica–epoxy vitrimer nanocomposites, *Macromolecules* 49 (2016) 5893–5902.
- [8] M. Delahaye, J.M. Winne, F.E. Du Prez, Internal catalysis in covalent adaptable networks: phthalate monoester transesterification as a versatile dynamic cross-linking chemistry, *J. Am. Chem. Soc.* 141 (2019) 15277–15287.
- [9] H. Zhang, S. Majumdar, R.A.T.M. van Benthem, R.P. Sijbesma, J.P.A. Heuts, Intramolecularly catalyzed dynamic polyester networks using neighboring carboxylic and sulfonic acid groups, *ACS Macro Lett.* 9 (2020) 272–277.
- [10] M. Podgorski, S. Mavila, S. Huang, N. Spurgin, J. Sinha, C.N. Bowman, Thiol-anhydride dynamic reversible networks, *Angew. Chem. Int. Ed. Engl.* 59 (2020) 9345–9349.
- [11] W. Denissen, G. Rivero, R. Nicolay, L. Leibler, J.M. Winne, F.E. Du Prez, Vinylogous urethane vitrimers, *Adv. Funct. Mater.* 25 (2015) 2451–2457.
- [12] W. Denissen, M. Droysbeke, R. Nicolay, L. Leibler, J.M. Winne, F.E. Du Prez,

- Chemical control of the viscoelastic properties of vinyllogous urethane vitrimers, *Nat. Commun.* 8 (2017) 14857.
- [13] W. Denissen, I. De Baere, W. Van Paepegem, L. Leibler, J. Winne, F.E. Du Prez, Vinyllogous urea vitrimers and their application in fiber reinforced composites, *Macromolecules* 51 (2018) 2054–2064.
- [14] M. Guerre, C. Taplan, R. Nicolay, J.M. Winne, F.E. Du Prez, Fluorinated vitrimer elastomers with a dual temperature response, *J. Am. Chem. Soc.* 140 (2018) 13272–13284.
- [15] M.M. Obadia, B.P. Mudraboyina, A. Serghei, D. Montarnal, E. Drockenmuller, Reprocessing and recycling of highly cross-linked ion-conducting networks through transalkylation exchanges of C-N bonds, *J. Am. Chem. Soc.* 137 (2015) 6078–6083.
- [16] N. Zheng, Z. Fang, W. Zou, Q. Zhao, T. Xie, Thermoset shape-memory polyurethane with intrinsic plasticity enabled by transcarbamoylation, *Angew. Chem. Int. Ed.* 55 (2016) 11421–11425.
- [17] D.J. Fortman, J.P. Brutman, C.J. Cramer, M.A. Hillmyer, W.R. Dichtel, Mechanically activated, catalyst-free polyhydroxyurethane vitrimers, *J. Am. Chem. Soc.* 137 (2015) 14019–14022.
- [18] Y.X. Lu, Z. Guan, Olefin metathesis for effective polymer healing via dynamic exchange of strong carbon-carbon double bonds, *J. Am. Chem. Soc.* 134 (2012) 14226–14231.
- [19] Y.-X. Lu, F. Tournilhac, L. Leibler, Z. Guan, Making insoluble polymer networks malleable via olefin metathesis, *J. Am. Chem. Soc.* 134 (2012) 8424–8427.
- [20] P. Taynton, K. Yu, R.K. Shoemaker, Y. Jin, H.J. Qi, W. Zhang, Heat- or water-driven malleability in a highly recyclable covalent network polymer, *Adv. Mater.* 26 (2014) 3938–3942.
- [21] S. Wang, S. Ma, Q. Li, X. Xu, B. Wang, W. Yuan, S. Zhou, S. You, J. Zhu, Facile in situ preparation of high-performance epoxy vitrimer from renewable resources and its application in nondestructive recyclable carbon fiber composite, *Green Chem.* 21 (2019) 1484–1497.
- [22] S. Wang, S. Ma, Q. Li, W. Yuan, B. Wang, J. Zhu, Robust, fire-safe, monomer-recovery, highly malleable thermosets from renewable bioresources, *Macromolecules* 51 (2018) 8001–8012.
- [23] J.M. Matxain, J.M. Asua, F. Ruiperez, Design of new disulfide-based organic compounds for the improvement of self-healing materials, *Phys. Chem. Chem. Phys.* 18 (2016) 1758–1770.
- [24] R. Martin, A. Rekondo, A. Ruiz de Luzuriaga, G. Cabañero, H.J. Grande, I. Odriozola, The processability of a poly(urea-urethane) elastomer reversibly crosslinked with aromatic disulfide bridges, *J. Mater. Chem. A* 2 (2014) 5710–5715.
- [25] X. Wu, X. Yang, W. Huang, R. Yu, X. Zhao, Y. Zhang, A facile access to stiff epoxy vitrimer with excellent mechanical properties via siloxane equilibration, *J. Mater. Chem. A* 6 (2018) 10184–10188.
- [26] Y. Nishimura, J. Chung, H. Muradyan, Z. Guan, Silyl ether as a robust and thermally stable dynamic covalent motif for malleable polymer design, *J. Am. Chem. Soc.* 139 (2017) 14881–14884.
- [27] C.A. Tretbar, J.A. Neal, Z. Guan, Direct silyl ether metathesis for vitrimers with exceptional thermal stability, *J. Am. Chem. Soc.* 141 (2019) 16595–16599.
- [28] H. Ying, Y. Zhang, J. Cheng, Dynamic urea bond for the design of reversible and self-healing polymers, *Nat. Commun.* 5 (2014) 3218.
- [29] W.A. Ogden, Z. Guan, Recyclable, strong, and highly malleable thermosets based on boroxine networks, *J. Am. Chem. Soc.* 140 (2018) 6217–6220.
- [30] M. Röttger, T. Domenech, R. van der Weegen, A. Breuillac, R. Nicolay, L. Leibler, High-performance vitrimers from commodity thermoplastics through dioxaborolane metathesis, *Science* 356 (2017) 62–65.
- [31] J.C. Grim, T.E. Brown, B.A. Aguado, D.A. Chapnick, A.L. Viert, X. Liu, K.S. Anseth, A reversible and repeatable thiol-ene bioconjugation for dynamic patterning of signaling proteins in hydrogels, *ACS Central Sci.* 4 (2018) 909–916.
- [32] H. Lei, S. Wang, D.J. Liaw, Y. Cheng, X. Yang, J. Tan, X. Chen, J. Gu, Y. Zhang, Tunable and processable shape-memory materials based on solvent-free, catalyst-free polycondensation between formaldehyde and diamine at room temperature, *ACS Macro Lett.* 8 (2019) 582–587.
- [33] Q. Chen, Y. Wei, Y. Ji, Photo-responsive liquid crystalline vitrimer containing oligoanilines, *Chin. Chem. Lett.* 28 (2017) 2139–2142.
- [34] N. Van Herck, D. Maes, K. Unal, M. Guerre, J.M. Winne, F.E. Du Prez, Covalent adaptable networks with tunable exchange rates based on reversible thiol-yne cross-linking, *Angew. Chem. Int. Ed.* 59 (2020) 3609–3617.
- [35] P.R. Christensen, A.M. Scheuermann, K.E. Loeffler, B.A. Helms, Closed-loop recycling of plastics enabled by dynamic covalent diketoenamine bonds, *Nat. Chem.* 11 (2019) 442–448.
- [36] Q. Li, S. Ma, S. Wang, W. Yuan, X. Xu, B. Wang, K. Huang, J. Zhu, Facile catalyst-free synthesis, exchanging, and hydrolysis of an acetal motif for dynamic covalent networks, *J. Mater. Chem. A* 7 (2019) 18039–18049.
- [37] Q. Li, S. Ma, S. Wang, Y. Liu, M.A. Taher, B. Wang, K. Huang, X. Xu, Y. Han, J. Zhu, Green and facile preparation of readily dual-recyclable thermosetting polymers with superior stability based on asymmetric acetal, *Macromolecules* 53 (2020) 1474–1485.
- [38] X. Xu, S. Ma, S. Wang, J. Wu, Q. Li, N. Lu, Y. Liu, J. Yang, J. Feng, J. Zhu, Dihydrazone-based dynamic covalent epoxy networks with high creep resistance, controlled degradability, and intrinsic antibacteria from bioresources, *J. Mater. Chem. A* 8 (2020) 11261–11274.
- [39] D.J. Fortman, J.P. Brutman, G.X. De Hoe, R.L. Snyder, W.R. Dichtel, M.A. Hillmyer, Approaches to sustainable and continually recyclable cross-linked polymers, *ACS Sustain. Chem. Eng.* 6 (2018) 11145–11159.
- [40] B. Zhang, K. Kowsari, A. Serjouei, M.L. Dunn, Q. Ge, Reprocessable thermosets for sustainable three-dimensional printing, *Nat. Commun.* 9 (2018) 1831.
- [41] T. Liu, C. Hao, L. Wang, Y. Li, W. Liu, J. Xin, J. Zhang, Eugenol-derived biobased epoxy: shape memory, repairing, and recyclability, *Macromolecules* 50 (2017) 8588–8597.
- [42] Y. Yang, E.M. Terentjev, Y. Wei, Y. Ji, Solvent-assisted programming of flat polymer sheets into reconfigurable and self-healing 3D structures, *Nat. Commun.* 9 (2018) 1906.
- [43] Y. Yang, Z. Pei, X. Zhang, L. Tao, Y. Wei, Y. Ji, Carbon nanotube-vitrimer composite for facile and efficient photo-welding of epoxy, *Chem. Sci.* 5 (2014) 3486–3492.
- [44] T. Liu, S. Zhang, C. Hao, C. Verdi, W. Liu, H. Liu, J. Zhang, Glycerol induced catalyst-free curing of epoxy and vitrimer preparation, *Macromol. Rapid Commun.* 40 (2019) 1800889.
- [45] J. Han, T. Liu, C. Hao, S. Zhang, B. Guo, J. Zhang, A catalyst-free epoxy vitrimer system based on multifunctional hyperbranched polymer, *Macromolecules* 51 (2018) 6789–6799.
- [46] F.I. Altuna, V. Pettarin, R.J.J. Williams, Self-healable polymer networks based on the cross-linking of epoxidised soybean oil by an aqueous citric acid solution, *Green Chem.* 15 (2013) 3360–3366.
- [47] T. Ube, K. Kawasaki, T. Ikeda, Photomobile liquid-crystalline elastomers with rearrangeable networks, *Adv. Mater.* 28 (2016) 8212–8217.
- [48] F.I. Altuna, C.E. Hoppe, R.J.J. Williams, Epoxy vitrimers with a covalently bonded tertiary amine as catalyst of the transesterification reaction, *Eur. Polym. J.* 113 (2019) 297–304.
- [49] Y. Li, T. Liu, S. Zhang, L. Shao, M. Fei, H. Yu, J. Zhang, Catalyst-free vitrimer elastomers based on a dimer acid: robust mechanical performance, adaptability and hydrothermal recyclability, *Green Chem.* 22 (2020) 870–881.
- [50] H. Zhang, X. Xu, Improving the transesterification and electrical conductivity of vitrimers by doping with conductive polymer wrapped carbon nanotubes, *Compos. Part A-Appl. S.* 99 (2017) 15–22.
- [51] M. Bhagiylakshmi, S. Vishnu Priya, J. Herbert Mabel, M. Palanichamy, V. Murugesan, Effect of hydrophobic and hydrophilic properties of solid acid catalysts on the esterification of maleic anhydride with ethanol, *Catal. Commun.* 9 (2008) 2007–2012.
- [52] S. Ma, D.C. Webster, F. Jabeen, Hard and flexible, degradable thermosets from renewable bioresources with the assistance of water and ethanol, *Macromolecules* 49 (2016) 3780–3788.
- [53] Q. Li, Y. Zhou, X. Hang, S. Deng, F. Huang, L. Du, Z. Li, Synthesis and characterization of a novel arylacetylene oligomer containing POSS units in main chains, *Eur. Polym. J.* 44 (2008) 2538–2544.
- [54] Z. Zhang, G. Liang, P. Ren, J. Wang, Curing behavior of epoxy/POSS/DDS hybrid systems, *Polym. Compos.* 29 (2008) 77–83.
- [55] S. Wang, S. Ma, C. Xu, Y. Liu, J. Dai, Z. Wang, X. Liu, J. Chen, X. Shen, J. Wei, J. Zhu, Vanillin-derived high-performance flame retardant epoxy resins: facile synthesis and properties, *Macromolecules* 50 (2017) 1892–1901.
- [56] S. Ma, D.C. Webster, Naturally occurring acids as cross-linkers to yield VOC-free, high-performance, fully bio-based degradable thermosets, *Macromolecules* 48 (2015) 7127–7137.
- [57] W. Yuan, S. Ma, S. Wang, Q. Li, B. Wang, X. Xu, K. Huang, J. Chen, S. You, J. Zhu, Synthesis of fully bio-based diepoxy monomer with dicyclo diacetal for high-performance, readily degradable thermosets, *Eur. Polym. J.* 117 (2019) 200–207.
- [58] P. Li, S. Ma, J. Dai, X. Liu, Y. Jiang, S. Wang, J. Wei, J. Chen, J. Zhu, Itaconic acid as a green alternative to acrylic acid for producing a soybean oil-based thermoset: synthesis and properties, *ACS Sustain. Chem. Eng.* 5 (2017) 1228–1236.
- [59] L. Lu, J. Pan, G. Li, Recyclable high-performance epoxy based on transesterification reaction, *J. Mater. Chem. A* 5 (2017) 21505–21513.
- [60] M. Hayashi, R. Yano, A. Takasu, Synthesis of amorphous low Tg polyesters with multiple COOH side groups and their utilization for elastomeric vitrimers based on post-polymerization cross-linking, *Polym. Chem.* 10 (2019) 2047–2056.
- [61] L. Imbernon, S. Norvez, L. Leibler, Stress relaxation and self-adhesion of rubbers with exchangeable links, *Macromolecules* 49 (2016) 2172–2178.
- [62] M. Guerre, C. Taplan, J.M. Winne, F.E. Du Prez, Vitrimers: directing chemical reactivity to control material properties, *Chem. Sci.* 11 (2020) 4855–4870.
- [63] C. Taplan, M. Guerre, J.M. Winne, F.E. Du Prez, Fast processing of highly cross-linked, low-viscosity vitrimers, *Mater. Horiz.* 7 (2020) 104–110.
- [64] M. Guerre, C. Taplan, R. Nicolay, J.M. Winne, F.E. Du Prez, Fluorinated vitrimer elastomers with a dual temperature response, *J. Am. Chem. Soc.* 140 (2018) 13272–13284.